

MODELING TRANSITING CIRCUMSTELLAR DISKS: CHARACTERIZING THE NEWLY DISCOVERED
ECLIPSING DISK SYSTEM OGLE LMC-ECL-11893ERIN L. SCOTT¹, ERIC E. MAMAJEK¹, MARK J. PECAUT^{1,2}, ALICE C. QUILLEN¹, FRED MOOLEKAMP¹, AND CAMERON P. M. BELL¹*submitted to Astrophysical Journal*

ABSTRACT

We investigate the nature of the unusual eclipsing star OGLE LMC-ECL-11893 (OGLE J05172127-6900558) in the Large Magellanic Cloud recently reported by Dong *et al.* The eclipse period for this star is 468 days, and the eclipses exhibit a minimum of ~ 1.4 mag, preceded by a plateau of ~ 0.8 mag. Spectra and optical/IR photometry are consistent with the eclipsed star being a lightly reddened B9III star of inferred age ~ 150 Myr and mass $\sim 4 M_{\odot}$. The disk appears to have an outer radius of ~ 0.2 AU with predicted temperatures of ~ 1100 - 1400 K. We model the eclipses as being due to either a transiting geometrically thin dust disk or gaseous accretion disk around a secondary object; the debris disk produces a better fit. We speculate on the origin of such a dense circumstellar dust disk structure orbiting a relatively old low-mass companion, and on the similarities of this system to the previously discovered EE Cep.

Subject headings: binaries: eclipsing – stars: individual (OGLE-LMC-ECL-11893)

1. INTRODUCTION

In the discovery paper for the eclipsing circum-secondary disk system orbiting 1SWASP J140747.93-394542.6, Mamajek *et al.* (2012) explored the possibility of finding other such systems, calculating the probability to be nonnegligible given continuous monitoring of a large number of young stars. Examples of eclipsing disks are notably rare, including famous examples of ϵ Aur, EE Cep, and OGLE-LMC-ECL-17782 (e.g., Kloppenborg *et al.* 2010; Galan *et al.* 2012; Graczyk *et al.* 2011), and recent surveys have yielded few, if any, candidates (e.g., Meng *et al.* 2014). Modeling of eclipsing disks can provide constraints on the geometry and structure of circumstellar disks—details which are difficult to constrain from spectral energy distributions alone.

OGLE 11893 (OGLE J05172127-6900558 = LMC SC8 354550; hereafter “OGLE 11893”)³ was first cataloged as a LMC member by Udalski *et al.* (2000), flagged as a variable by Zebrun *et al.* (2001), and classified as an eclipsing variable by Graczyk *et al.* (2011). Dong *et al.* (2014) first reported OGLE 11893 to be a particularly unusual eclipsing binary with a long period, deep eclipse, and asymmetric shape. Dong *et al.* (2014) proposed that the eclipses could be due to a transiting circumstellar disk. The properties of OGLE 11893 are compiled in Table 1. The eclipses are a repeating phenomenon, with a period of 468 days and depth of ~ 1.4 mag (Graczyk *et al.* 2011; Dong *et al.* 2014). The phase-folded light curve reveals an eclipse structure that is highly consistent on the timescale over which the star has been observed (~ 17 yr, ~ 13 orbital periods; Dong *et al.* 2014), indi-

cating that the disk is not precessing at a detectable rate. Dong *et al.* (2014) reported preliminary observations from the H α line profile that the star appears to be a Ae/Be star exhibiting H α emission.

In this contribution, we further characterize OGLE 11893 and model its eclipses using circumstellar disk models. In Section 2 we discuss observations for the star. In Section 3 we analyze the properties of OGLE 11893 and its light curve, and model the eclipses as due to various flavors of disks. In Section 4 we summarize our findings regarding the eclipsing disk.

2. DATA

2.1. Photometry

In order to model the light curve, we used data from the photometric observations of the OGLE-II and OGLE-III surveys, spanning 12 yr in total. The OGLE-II survey took place from 1996 December to 2000 November, using standard *V* and *I* photometric bands and generating 300-500 frames per field in *I* (Wyrzykowski *et al.* 2009). OGLE-III took place from 2001 July to 2009 May and produced a total of 866 photometric points for OGLE 11893 in *I* band and 61 points in *V* over the course of 8 yr (Graczyk *et al.* 2011). Further details on the star can be found in Dong *et al.* (2014) and in Table 1.

2.2. Spectroscopy

We analyze the blue optical spectrum of OGLE-LMC-ECL-11893 (Figure 1) presented in Dong *et al.* (2014), taken by J. Prieto on UT 2011 December 23 with the IMACS (Inamori-Magellan Areal Camera & Spectrograph; Dressler *et al.* 2006) instrument on the Baade 6.5 m telescope at Las Campanas Observatory. The blue spectrum was taken with the long 0".7 slit and 300 L mm⁻¹ grism, and yielded resolution $R \sim 1800$ between $\lambda\lambda$ 3500-6574 Å. The S/N of the IMACS blue spectrum is ~ 22 ($\sim 5000\text{\AA}$). Further details are described in Section 2 of Dong *et al.* (2014).

elscott@pas.rochester.edu

¹ Department of Physics and Astronomy, University of Rochester, Rochester, NY 14627-0171, USA² Physics Department, Rockhurst University, 1100 Rockhurst Road, Kansas City, MO 64110, USA³ The Optical Gravitational Lensing experiment, <http://ogle.astrouw.edu.pl/> (Udalski *et al.* 2000).

Table 1
Data for OGLE LMC-ECL-11893

(1) Parameter	(2) Value	(3) Units	(4) Ref.
α (ICRS)	05:17:21.27	h:m:s	Udalski et al. (2000)
δ (ICRS)	-69:00:55.8	d:m:s	Udalski et al. (2000)
Spec. Type	B9III:	...	This paper
U	17.854 ± 0.060	mag	Zaritsky et al. (2004)
B	17.954 ± 0.021	mag	Udalski et al. (2000)
V	17.753 ± 0.01	mag	Graczyk et al. (2011)
I_c	17.556 ± 0.01	mag	Graczyk et al. (2011)
J	17.61 ± 0.04	mag	Kato et al. (2007)
H	17.39 ± 0.10	mag	Kato et al. (2007)
K_s	17.43 ± 0.23	mag	Kato et al. (2007)
[3.6]	16.932 ± 0.107	mag	Meixner et al. (2006)
[4.5]	16.955 ± 0.104	mag	Meixner et al. (2006)
Period	468.045440	day	Graczyk et al. (2011)
Epoch(min.,HJD)	2454011.5436	day	Graczyk et al. (2011)
Dist. Mod.(LMC)	18.48 ± 0.05	mag	Walker (2012)
R_V (LMC)	3.41 ± 0.06	...	Gordon et al. (2003)
T_{eff}	12000 ± 300	K	This paper
$E(B - V)$	0.28 ± 0.02	mag	This paper
A_V	0.91 ± 0.06	mag	This paper
M_V	-1.64 ± 0.08	mag	This paper
M_{bol}	-2.32 ± 0.10	mag	This paper
$\log(L/L_{\odot})$	2.83 ± 0.04	dex	This paper
Radius	6.03 ± 0.42	R_{\odot}	This paper
Mass	~ 4.1	M_{\odot}	This paper
Age	~ 150	Myr	This paper

Note. — We assume ± 0.01 mag uncertainty in the mean out-of-eclipse V and I magnitudes from Graczyk et al. (2011); [3.6] and [4.5] *Spitzer* IRAC photometry is from the SAGE survey (Meixner et al. 2006) catalog accessible via Vizier at: <http://vizier.cfa.harvard.edu/viz-bin/Cat?II/305>.

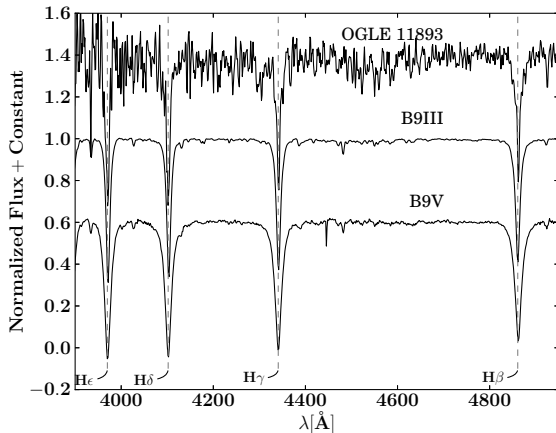


Figure 1. Comparison of the IMACS spectrum of OGLE 11893 to that of spectral standards HD 141774 (B9 V) and γ Lyr (B9 III). Here the B9 V standard is HD 141774 (Garrison & Schild 1979) and the B9 III standard is γ Lyr (Johnson & Morgan 1953).

3. ANALYSIS

3.1. Light Curve

Figure 2 shows the phase-folded light curve of OGLE 11893. The light curve shows a dimming of ~ 0.8 mag over ~ 8 days, which deepens to ~ 1.4 mag before returning to full brightness. The total duration of the eclipse is ~ 16 days. As we will show, this pattern is consistent with a disk that is nearly edge-on to the observer's line of sight, and which has a cleared inner region.

3.2. Spectral Classification

As shown in Figure 1, through comparison of the IMACS spectrum of OGLE 11893 to a grid of Galactic MK standards (Morgan & Keenan 1973) observed at a resolution of 4.3\AA with the RC spectrograph on the SMARTS 1.5 m telescope, we find that the Balmer lines are consistent with that of a B9 giant star. The luminosity class, however, is still somewhat uncertain due to the low S/N of the spectrum.

3.3. Reddening

We estimate the reddening by comparing to examples of unreddened Galactic late B-type giants. Garrison & Gray (1994) classified 10 stars as B9III or variant. Of those stars, the revised *Hipparcos* parallaxes of van Leeuwen (2007) only place two within 100 pc (and hence negligibly reddened): HD 145389 and HD 129174. Using the van Leeuwen (2007) parallaxes, and *UBV* photometry from Mermilliod (1997), we estimate their mean properties as $(B - V)_0 \simeq -0.09 \pm 0.03$, $(U - B)_0 \simeq -0.329 \pm 0.10$, $M_V \simeq 0.20 \pm 0.08$. Based solely on comparison of OGLE 11893's spectral type and colors in Table 1 to those of these well-studied nearby B9 III templates, we would expect $E(B - V) \simeq 0.29 \pm 0.05$, $A_V \simeq 0.94 \pm 0.17$ (assuming $E(B - V) - A_V$ relation of Olson 1975), and distance modulus $(m - M)_0 \simeq 16.6$. Hence if it were comparable to Galactic B9 III stars, we would predict a distance of ~ 21 kpc (well short of the LMC's distance of ~ 50 kpc; Walker 2012). The reddening is somewhat larger than predicted for the star's position in the LMC.

We can also estimate the intrinsic color of the B-type

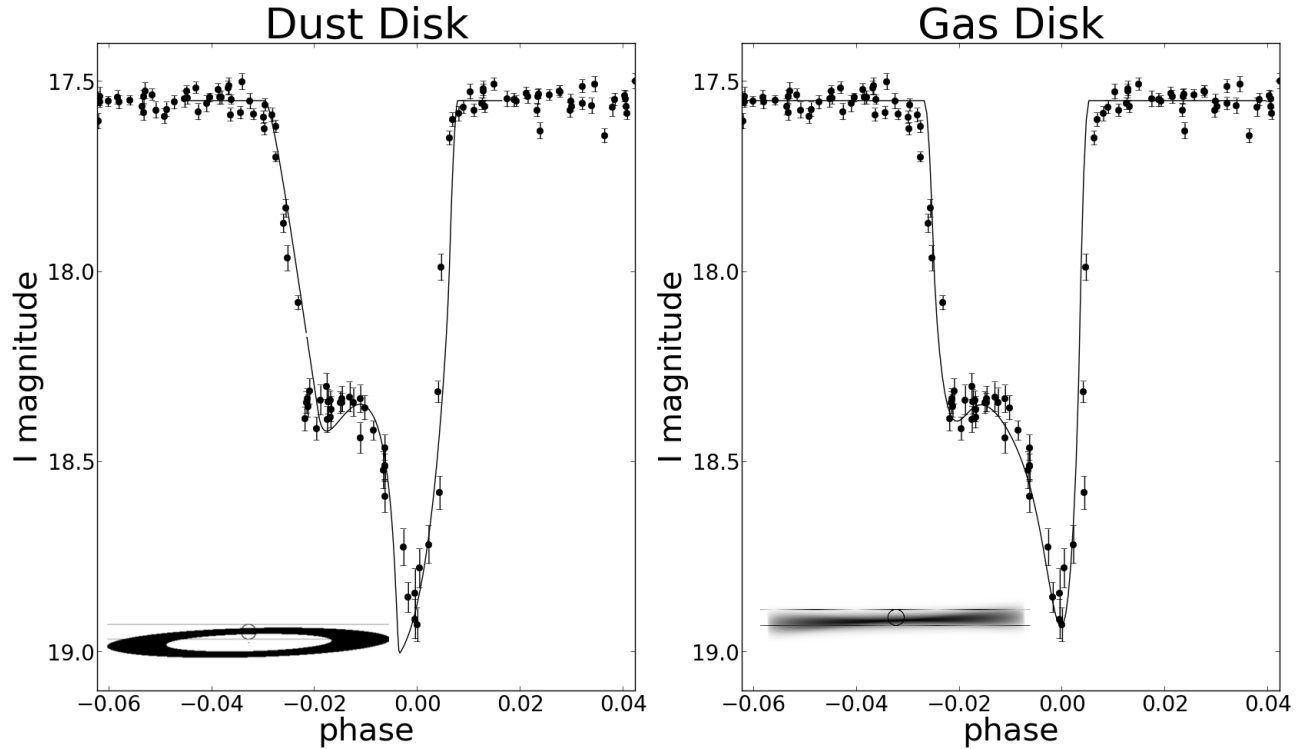


Figure 2. Phase-folded light curve for OGLE 11893 with best-fit synthetic light curves for (*left*) an infinitely thin dusty debris disk, and (*right*) flared gas-rich disk. Parameters of best fit synthetic light curves are compiled in Table 2.

star using the Q -method with the observed UBV photometry. We assume that the star suffers visual reddening similar to that of the Galactic average value ($E(U-B)/E(B-V) = 0.72$; Johnson & Morgan 1953), which is statistically consistent with values derived for hot stars in the LMC not near the 30 Dor complex (Walker & Morris 1968; Fitzpatrick 1986; Gordon et al. 2003). Using the revised calibration of Q versus spectral type for Be stars from Halbedel (1993), and the observed colors (see Table 1; $U-B = -0.10 \pm 0.06$, $B-V \simeq 0.20 \pm 0.04$), we estimate the star to have $Q = -0.245$ and a photometric spectral type of B8.3e. Unfortunately Halbedel (1993) does not provide the intrinsic colors for the Be stars. However, if we adopt the intrinsic color sequence for B stars from Pecaut & Mamajek (2013), the dereddened photometry corresponds to $(B-V)_0 = -0.095$, $(U-B)_0 = -0.314$, $E(B-V) = 0.296$. According to the updated spectral type-effective temperature relations of Pecaut & Mamajek (2013), for a Galactic main sequence star, this would correspond to a \sim B8 star with $T_{\text{eff}} \simeq 12100$ K.

The foreground Galactic reddening to the LMC varies from $E(B-V) \simeq 0.04$ -0.09 (Bessell 1991). Typical reddenings for hot stars in the LMC are $E(B-V) \simeq 0.15$ -0.31 mag (Gordon et al. 2003), consistent with what we see for OGLE 11893. However this is at odds with the extinction inferred from analyses of LMC RR Lyraes and red clump giants (Pejcha & Stanek 2009; Haschke et al. 2011), which yield $E(V-I_c) = 0.153$ and 0.070, respectively, in the vicinity of OGLE 11893 (corresponding to $A_V \simeq 0.38$ and 0.17, adopting $A_V/E(V-I_c) = 2.49$;

Stanek 1996). So while OGLE 11893 appears to have a typical reddening compared to hot stars studied in the LMC, it appears to be anomalously redder compared to that predicted from reddening maps of particular classes of star (e.g. RR Lyraes).

Using the SED fitting routine described in Pecaut & Mamajek (2013), we fit the $UBVIJHK_s$ photometry of OGLE 11893 through comparison to a grid of colors of Galactic B-type dwarfs of varying $E(B-V)$ (assuming a Galactic reddening curve). The best fit SED was for a star with $(B-V)_0 = -0.093$, $E(B-V) = 0.260$ mag, $A_V = 0.84$ mag, and $T_{\text{eff}} \simeq 11800$ K. These values are similar to what was previously derived using the Q -method.

3.4. HR Diagram Position

Based on the spectrum and photometry, we adopt for this star $T_{\text{eff}} \simeq 12000 \pm 300$ K, with reddening $E(B-V) = 0.28 \pm 0.02$ mag, extinction $A_V = 0.91 \pm 0.06$ mag. Adopting the mean LMC distance modulus from Walker (2012) of 18.48 ± 0.04 mag ($\varpi = 0.0201 \pm 0.0004$ mas), and a T_{eff} -appropriate bolometric correction from Code et al. (1976) of $BC_V = -0.68 \pm 0.06$ mag, we derive $M_V = -1.64 \pm 0.08$, $M_{\text{bol}} = -2.32 \pm 0.10$, $\log(L/L_\odot) = 2.83 \pm 0.04$, and radius $6.03 \pm 0.42 R_\odot$.

3.5. Age and Primary Mass

In order to estimate an age and mass based on HR diagram position, we use the PARAM 1.2 program,⁴

⁴ <http://stev.oapd.inaf.it/cgi-bin/param>

which uses the Bressan et al. (2012) evolutionary tracks. Adopting $T_{\text{eff}} = 12000 \pm 300$ K, $[\text{Fe}/\text{H}] = -0.3 \pm 0.05$ dex (typical for LMC; Luck et al 1998), $V_o = 16.84 \pm 0.06$ mag, and LMC parallax from Walker (2012), and assuming Bayesian priors of a Chabrier (2001) lognormal IMF and constant star-formation rate, PARAM 1.2 estimates the following a posteriori stellar parameters: age 154 ± 8 Myr, mass $= 4.09 \pm 0.14 M_{\odot}$, $\log(g) = 3.50 \pm 0.02$ dex, radius $5.76 \pm 0.14 R_{\odot}$. Using the piecewise linear fit from Ekström et al. (2012), including rotation, we derive a main sequence lifetime of ~ 185 Myr, hence OGLE 11893 is closer to the end of its lifetime than the beginning.

Given a period of 468 days and a primary mass of $4.09 M_{\odot}$, if we assume that the mass of the secondary is negligible compared to the primary, the orbital separation of the secondary is approximately 1.7 AU. Using the eclipse duration and the orbital period, we infer that the radius of the disk is ~ 0.20 AU. The disk radius should be smaller than the Hill radius of the secondary, placing a lower limit on the mass of the secondary of $M_2 \simeq 3M_1(r_{\text{disk}}/a)^3 > 0.014 M_{\odot} \simeq 15 M_{\text{Jup}}$. Hence the disked secondary is almost certainly a star or brown dwarf rather than a giant planet. Given the high luminosity of the primary, we find that the equilibrium disk temperature due to the primary alone is probably $T_{\text{eq}} \simeq 1250$ K, not far below the sublimation temperatures of silicate dust.

3.6. Eclipse Modeling

The disk structure was analyzed using a code⁵ that uses a model to generate synthetic light curves for varying parameters. The object-oriented model is made up of a star, a secondary object, and a disk. The star, which is held at a fixed mass, is modeled as a spherical grid of points, each of which contains a fraction of the star's total flux, using the limb darkening values from van Hamme (1993). The secondary is modeled as a solid sphere. Our calculations show that the secondary is between 0.15 and $0.38 M_{\odot}$ (see Equations (12) and (3.6.2)). To calculate the secondary radius and temperature, we adopted an isochrone from Bressan et al. (2012), which covers mass ranges from 0.1 to $3.8 M_{\odot}$, adopting LMC composition $Y = 0.2572$, $Z = 0.0047$ for age 200 Myr.

These objects are put together into an orbital system, the parameters of which are the period and the inclination with respect to the observer's line of sight. To avoid degeneracy in the best-fit solution, we assume a perfectly circular orbit. The program then uses vector addition to determine whether any point on the star is eclipsed by any part of the secondary or disk as seen by the observer. The observed magnitude is then calculated and recorded.

To find a model that best fits the observed data, the program utilizes a simplex routine from Press et al. (1998) to minimize χ^2 . Due to a systematic variation in the error, which was consistently larger for dimmer points in the light curve, resulting in overfitting in the ingress and egress regions of the eclipse and underfitting in the central regions, all errors were set equal to the median value of 0.02 mag.

The free parameters are the orientation of the disk (θ_x and θ_y), the dimensions of the disk (R_{in} and R_{out}), and

the inclination of the orbit. If the model is of a flared gas disk rather than a flat dust disk, the inner radius is automatically set to the dust sublimation radius, but additional parameters are also allowed to vary: the density power law $1 \leq \alpha \leq 3$ (where $\rho \propto r^{-\alpha}$), the secondary mass $0.15 M_{\odot} \leq M_2 \leq 0.38 M_{\odot}$ whose bounds were determined by calculating the Hill radius (see Equations (10) and (12)), and the disk mass M_{disk} , which was varied on a logarithmic scale of $-2 \leq \gamma \leq -11$, where $\gamma = \log(M_{\text{disk}}/M_2)$. At the present time we are unable to constrain the mass opacity of the disk matter, so we adopt a realistic opacity from Miyake & Nakagawa (1993) of $\kappa = 0.1 \text{ m}^2 \text{ kg}^{-1}$ which would correspond to the V-band mass opacity of a population of compact dust particles with composition representative of interstellar dust, grain sizes between 10^{-8} and 10^{-1} m following a size^{-3.5} power-law distribution. Examination of the multi-band light curve from Dong et al. (2014) shows that the transiting dust appears to be consistent with $A_B/A_V \simeq 1.2$, which is close to that expected for a $R_V \simeq 5$ interstellar dust extinction curve Mathis (1990). The transiting dust is clearly not gray, and likely is reflecting a power-law distribution of dust grains down to submicron size, not too unlike an interstellar dust grains population.

3.6.1. Flat Dust Disk

The eclipse was first fit with the simplest model, an infinitely thin annulus. The best fit for this flat dust disk was found to be an inner radius of $R_{\text{in}} = 26.2 R_{\odot}$, an outer radius of $R_{\text{out}} = 45.8 R_{\odot}$, a disk tilt of $\theta_x = 2.0^\circ$, a disk obliquity of $\theta_y = 7.0^\circ$ from edge-on, an orbital inclination of $i = 89.38^\circ$, and a flat optical depth of $\tau_0 = 1.8$. This simple disk produced a model light curve that was a reasonable visual fit to the data, with χ^2/ν of $1186/113 = 10.5$.

A slightly more complex model for the debris disk allowed the optical depth to vary according to a power law, which produced a best fit model with $R_{\text{in}} = 26.1 R_{\odot}$, an outer radius of $R_{\text{out}} = 44.8 R_{\odot}$, a disk tilt of $\theta_x = 1.5^\circ$, a disk obliquity of $\theta_y = 5.9^\circ$ from edge-on, an orbital inclination of $i = 89.46^\circ$, and an optical depth of $\tau_0 = 7.9$ at the inner edge of the disk which varied according to a power law of $p = 0.6$. This model had $\chi^2/\nu = 1073.8/112 = 9.6$, and was a better overall fit to the data.

The infinitely thin debris disk model captures the overall light curve structure relatively well, but has some trouble matching the data in the central regions of the eclipse (see Figure 2).

3.6.2. Flared Gas and Dust Disk

Since the lack of detailed substructure indicates the possibility that the eclipses are due to a disk with non-negligible scale height, we next attempted to fit the light curve with a flared gas and dust disk model. Assuming vertical hydrostatic equilibrium, the scale height of such a disk is given by Shakura & Sunyaev (1973):

$$h(r) = \frac{c_s}{\Omega} \quad (1)$$

where c_s is the sound speed

$$c_s = \sqrt{\frac{k_b T(r)}{\mu m_H}} \quad (2)$$

⁵ Written by Fred Moolekamp, maintained and updated by Erin Scott (UR).

and, assuming circular Keplerian orbits, Ω is the rotation rate

$$\Omega = \sqrt{\frac{GM_2}{r^3}}, \quad (3)$$

which gives a scale height of

$$h(r) = \sqrt{\frac{k_b r^3 T(r)}{\mu m_H G M_2}}. \quad (4)$$

The temperature profile can be simplified for modeling purposes. Given the size of the disk, the outer disk is almost certainly dominated by heating from the primary star, as we discuss in Section 3.5, putting it at a temperature of $T_{\text{out}} \simeq 1100$ K. The inner edge of the disk is likely at the silicate dust sublimation temperature $T_{\text{in}} \simeq 1400$ K, as commonly seen among T Tauri disks (Muzerolle et al. 2003). Hence the radial variation in temperature throughout the disk is likely less than $\sim 25\%$. Since $h \propto T^{1/2}$, the scale height h likely varies by only order $\sim 15\%$ between the inner and outer radii. To simplify our calculations, we adopt $T = 1250$ K, which should translate to accuracy of scale heights $\sim 10\%$ – 15% over the whole disk.

For a roughly constant temperature, the density structure of a flared accretion disk can be modeled by a Gaussian curve (Shakura & Sunyaev 1973):

$$\rho(r, z) = \rho(r, 0) e^{z^2/2h(r)^2} \quad (5)$$

where $1 \leq \alpha \leq 3$. The midplane density ρ_0 is set so as to give the correct disk mass⁶ for a given value of α . Assuming that the temperature of the disk is constant, the density equation can be integrated:

$$M_{\text{disk}} = \int_{R_{\text{in}}}^{R_{\text{out}}} \int_{-\infty}^{\infty} \int_0^{2\pi} \rho_0 e^{z^2/2h(r)^2} \left(\frac{r}{R_2}\right)^{-\alpha} r dr d\phi dz \quad (6)$$

$$M_{\text{disk}} = 2\pi \rho_0 \int_{R_{\text{in}}}^{R_{\text{out}}} r \left(\frac{r}{R_2}\right)^{-\alpha} dr \int_{-\infty}^{\infty} e^{z^2/2h(r)^2} dz \quad (7)$$

$$M_{\text{disk}} = (2\pi)^{\frac{3}{2}} \rho_0 R_2^\alpha \int_{R_{\text{in}}}^{R_{\text{out}}} r^{1-\alpha} h(r) dr \quad (8)$$

$$M_{\text{disk}} = \frac{2(2\pi)^{3/2}}{7-2\alpha} \rho_0 R_2^\alpha [R_{\text{out}}^{2-\alpha} h(R_{\text{out}}) - R_{\text{in}}^{2-\alpha} h(R_{\text{in}})], \quad (9)$$

which can then be solved for ρ_0 .

In this model, the secondary mass becomes important, as it determines the structure of the disk. Though we lack radial velocity measurements and therefore do not have a precise mass value for the secondary, it is possible to constrain its mass by using the period and duration of the eclipse to put limits on the Hill radius, the point at which

⁶ The density calculation only accounts for the small dust grains that are the primary source of opacity. Gas and larger grains that contribute most of the mass, but are not a significant source of opacity, are not included in the calculation, resulting in a model disk mass that is orders of magnitude lower than the actual mass.

the gravitational influence of the secondary balances that of the primary. For a circular orbit,

$$r_H = a \left(\frac{\mu}{3}\right)^{\frac{1}{3}}, \quad (10)$$

where a is the semi-major axis and μ is the mass ratio $\mu \equiv M_2/(M_1 + M_2)$. The outer radius of a gas disk extends out to ξr_H , where estimates of ξ are typically between $\xi \sim 0.3$ (Ayliffe & Bate 2009) and 0.4 (Martin & Lubow 2011). The semi-major axis can be calculated using the orbital period and the mass of the primary, giving $a = 367 R_\odot = 1.7$ AU. The outer radius of the disk can be calculated from the ratio of the eclipse duration to the period

$$\frac{T_{\text{ecl}}}{P} = \frac{\Theta}{2\pi}, \quad (11)$$

where Θ is the angular distance traversed by the secondary/disk system during the eclipse.

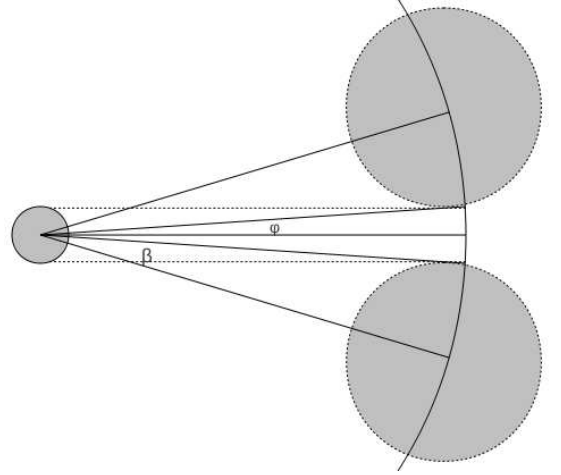


Figure 3. Schematic of the total angular distance traversed by the secondary/disk system over the duration of the eclipse. Since only a small fraction ($\sim 3\%$) of the period is taken up by the eclipse, the angles are small.

As seen in Figure 3, $\Theta = 2\varphi + 2\beta$. Since the eclipse-to-period ratio is small, we use the small angle approximation $\varphi \simeq \sin(\varphi) \simeq R_1/a$ and $\beta \simeq \sin(\beta) \simeq \xi r_H/a$, giving $\Theta = (2\xi r_H + 2R_1)/a$. Inserting this and Equation (10) into Equation (11), we obtain the cubic equation

$$\left(\xi^3 - 3\pi^3 \frac{T^3}{P^3}\right) M_2 + 3\xi^2 k^{\frac{1}{3}} M_2^{\frac{2}{3}} + 3\xi k^{\frac{2}{3}} M_2^{\frac{1}{3}} + k - 3\pi^3 \frac{T^3}{P^3} M_1 = 0, \quad (12)$$

where $k = 12\pi^2 R_1^3 / GP^2$. Solving for M_2 , we obtain bounds⁷ on the secondary mass of $M_2 = 0.23 M_\odot$ for $\xi = 0.4$ and $M_2 = 0.61 M_\odot$ for $\xi = 0.3$, assuming a circular orbit. In addition, the lack of a visible secondary eclipse puts an upper limit of $2.1 M_\odot$ on the mass of the secondary for this system's age and metallicity.

The best-fit result for a gas disk was an edge-on disk ($\theta_y = 0^\circ$) with an obliquity of $\theta_x = 0.9^\circ$, an orbital

⁷ The upper mass limit is not a hard limit, as a disk can potentially be smaller relative to the Hill radius of the secondary.

inclination of $i = 89.7^\circ$, an inner radius of $R_{\text{in}} = 2.4 R_\odot$, an outer radius of $R_{\text{out}} = 35.5 R_\odot$, a secondary mass of $M_2 = 0.32 M_\odot$, a radial density dropoff of $\alpha = 2.8$, and a disk mass of $\log(M_{\text{disk}}/M_2) = -7.8$. The best fit for a gas and dust rich model produced $\chi^2/\nu = 1322/112 = 11.8$. The best-fit parameters for both models are listed in Table 2.

3.6.3. Hybrid Disk

While both models show general agreement with the overall eclipse trend, both have problems fitting the finer details. Therefore, we attempted to see whether the fit could be improved by implementing a hybrid model that combined the flat dust disk and flared gas disk. The best fit for the hybrid model had an obliquity of $\theta_x = 1.1^\circ$, a tilt of $\theta_y = 3.0^\circ$, an orbital inclination of $i = 89.74^\circ$, an inner radius of $R_{\text{in}} = 16.7 R_\odot$, an outer radius of $R_{\text{out}} = 41.8 R_\odot$, a secondary mass of $M_2 = 1 M_\odot$, a radial density dropoff of $\alpha = 1$, a disk mass of $\log(M_{\text{disk}}/M_2) = -9$ dex, a debris disk optical depth of $\tau = 6.5$, and a debris disk density dropoff power law of $p = 1.5$, which gave $\chi^2/\nu = 1419/110 = 12.9$.

Setting the dust disk (which produced the better fit out of the two previous models) as the null model and the hybrid disk as the alternative model, we then used a likelihood ratio test to determine whether the hybrid model produced a statistically significant improvement in the fit. The likelihood function

$$L = \prod_{i=1}^n \left(\frac{1}{2\pi\sigma_i^2} \right)^{1/2} \exp \left(-\frac{1}{2} \left(\frac{y_i - y(x_i)}{\sigma_i} \right)^2 \right) \quad (13)$$

(Bevington & Robinson 1968) becomes

$$L = \left(\frac{1}{\pi\sigma^2} \right)^{n/2} \exp \left(-\frac{\chi^2}{2} \right) \quad (14)$$

when the errors of each data point are assumed homoskedastic. In order to evaluate whether the hybrid model produced a statistically significant improvement in the fit, we made use of the Bayesian Information Criterion (BIC)

$$\text{BIC} = -2\ln(L_{\text{max}}) + k\ln(N) = \chi^2 + k\ln(N) \quad (15)$$

(Liddle 2007; Schwarz 1978), where k is the number of free parameters, N is the number of data points, and L_{max} is the maximum likelihood. The dust and hybrid models were fit with 7 and 9 free parameters, respectively, to 120 data points, hence the dust and hybrid models had 112 and 110 free parameters, respectively. The best-fit debris disk model produces $\chi^2 = 1073.8$; therefore the hybrid model will have produced a statistically significant improvement only if it has a BIC lower than that produced by the dust disk model, or

$$\chi_{\text{hybrid}}^2 + 9\ln(120) < 1073.4 + 7\ln(120), \quad (16)$$

which gives $\chi_{\text{hybrid}}^2/\nu < 1064.2/110$ for the hybrid disk model. Since the best-fit hybrid model produced $\chi^2/\nu = 1073.8/110$, we conclude that the hybrid model does not produce a statistically significant improvement in the fit.

4. DISCUSSION

OGLE 11893 appears to be near the end of its main sequence life, and it is unlikely to have a companion that has retained its primordial protoplanetary disk. This leaves the possibility that the companion is surrounded by either a dusty debris disk or a second-generation gas-rich disk. The disk-eclipse system OGLE 11893 bears a strong resemblance to EE Cep, the only other known system discovered to date with a disk eclipsing a Be primary. Galan et al. (2012) speculate that the circumsecondary disk of EE Cep is fed by mass loss from the primary Be star, and given the similarity of the two systems, this is a possibility for OGLE 11893 as well.

The simplest flat debris disk model produced the best fit to the data (see Figure 2), with a χ^2/ν value of $1073.8/112 = 9.6$. Even the best-fit parameters reproduced the light curve poorly in the central region of the eclipse. Currently the primary is modeled as a perfect sphere even though it has the spectral signatures of a rapidly rotating Be star (Dong et al. 2014). Modifying the model star to account for the elongation and gravitational darkening at the equator due to its rapid rotation would be an important step in improving the model.

OGLE 11893 and other eclipsing systems like it can be used to learn more about the composition and geometry of circumstellar disks through continued modeling efforts and photometric and spectroscopic observations. The discovery of this system in addition to J1407 and EE Cep provides evidence that eclipsing circumsecondary disk systems may not be as rare as previously thought, and that both archival searches and long-term photometric monitoring of large areas of the sky are likely to uncover more of them.

E.L.S., E.E.M., and F.M. acknowledge support from NSF award AST-1313029. E.E.M. and M.J.P. acknowledge support from NSF AST-1008908. E.E.M., E.L.S., F.M., M.J.P., and C.P.M.B. acknowledge support from the University of Rochester College of Arts and Sciences. This research has made use of NASA ADS, Vizier, and SIMBAD, and data from the OGLE survey. This publication makes use of data products from the Two Micron All Sky Survey, which is a joint project of the University of Massachusetts and the Infrared Processing and Analysis Center/California Institute of Technology, funded by the National Aeronautics and Space Administration and the National Science Foundation. The authors thank Subo Dong, Jose Prieto, Szymon Kozlowski, and Matt Kenworthy for discussions, and we thank the referee for a thoughtful and timely report.

REFERENCES

- Ayliffe, B. A. & Bate, M. R. 2009, MNRAS, 397, 657
- Bessell, M. S. 1991, A&A, 242, L17
- Bevington, P. R. & Robinson, D. K. 1968, Data Reduction and Error Analysis for the Physical Sciences (2nd ed.; New York, NY: McGraw-Hill, Inc.), 144
- Bressan, A., Marigo, P., Girardi, L., et al. 2012, MNRAS, 427, 127
- Chabrier, G. 2001, ApJ, 554, 1274
- Code, A. D., Bless, R. C., Davis, J., & Brown, R. H. 1976, ApJ, 203, 417
- Dong, S., Katz, B., Prieto, J. L., et al., 2014, ApJ, 788, 41
- Dressler, A., Hare, T., Bigelow, B. C., & Osip, D. J. 2006, Proc. SPIE, 6269

Table 2
Best Eclipse Fits for OGLE LMC-ECL-11893

(1) Parameter	(2) Dust Disk	(3) Gas Disk	(4) Hybrid Disk	(5) Units
θ_x	1.5	0.9	1.1	deg
θ_y	5.9	0.0	3.0	deg
i	89.46	89.70	89.74	deg
R_{in}	26.1	2.8	16.7	R_{\odot}
R_{out}	44.8	35.5	41.8	R_{\odot}
α	—	2.8	1.0	...
M_2	0.12	0.32	1.00	M_{\odot}
$\log(M_{\text{disk}}/M_2)$	-6.9	-7.8	-9.0	dex
κ	0.1	0.1	0.1	$\text{m}^2 \text{kg}^{-1}$
τ_0	7.9	—	6.5	...
p	0.6	—	1.5	...
χ^2/ν	1073.8 / 112	1322 / 112	1419 / 110	...

Note. — Final best-fit parameters for the dust disk and gas disk models. M_2 and M_{disk} were only varied in the gas disk model. In the dust disk model, secondary mass was held fixed and M_{disk} was calculated using the assigned opacity and the best-fit values of the disk dimensions.

- Ekström, S., Georgy, C., Eggenberger, P., et al. 2012, *A&A*, 537, 18
- Fitzpatrick, E. L. 1986, *AJ*, 92, 1068
- Gałań, C., Mikołajewski, M., Tomov, T., et al. 2012, *A&A*, 544, A53
- Garrison, R. F., & Gray, R. O. 1994, *AJ*, 107, 1556
- Garrison, R. F., & Schild, R. E. 1979, *AJ*, 84, 1020
- Gordon, K. D., Clayton, G. C., Misselt, K. A., et al. 2003, *ApJ*, 594, 279
- Graczyk, D., Soszynski, I., Poleski, R., et al. 2011, *Acta Astronomica*, 61, 103
- Halbedel, E. M. 1993, *PASP*, 105, 465
- Haschke, R., Grebel, E. K., & Duffau, S. 2011, *AJ*, 141, 158
- Johnson, H. L., & Morgan, W. W. 1953, *ApJ*, 117, 313
- Kato, D., Nagashima, C., Nagayama, T., et al. 2007, *PASJ*, 59, 615
- Kloppenborg, B., Stencel, R., Monnier, J. D., et al. 2010, *Nature*, 464, 870
- Liddle, A. R. 2007, *MNRAS*, 377, L74
- Luck, R. E., Moffett, T. J., Barnes, T. G. III, & Gieren, W. P. 1998, *AJ*, 115, 605
- Mamajek, E. E., Quillen, A. C., Peca, M. J., et al. 2012, *AJ*, 143, 72
- Martin, R. G. & Lubow, S. H. 2011, *MNRAS*, 413, 1447
- Mathis, J. S. 1990, *ARA&A*, 28, 37
- Meixner, M., Gordon, K. D., Indebetouw, R., et al. 2006, *AJ*, 132, 2268
- Meng, Z., Quillen, A. C., Bell, C., & Scott, E. L. 2014, *MNRAS*, 441, 4
- Mermilliod, J. C. 1997, *yCat*, 2168, 0
- Miyake, K. & Nakagawa, Y. 1993, *Icar*, 106, 20
- Morgan, W. W., & Keenan, P. C. 1973, *ARA&A*, 11, 29
- Muzerolle, J., Calvet, N., Hartmann, L., & D'Alessio, P. 2003, *ApJ*, 597, L149
- Olson, B. I. 1975, *PASP*, 87, 349
- Peca, M., & Mamajek, E. E. 2013, *ApJS*, 208, 9
- Pejcha, O., & Stanek, K. Z. 2009, *ApJ*, 704, 1730
- Press, W. H., Teulolsky, S. A., Vetterling, W. T., & Flannery, B. P. 1992, *Numerical Recipes in C: The Art of Scientific Computing* (New York, NY: Cambridge Univ. Press)
- Schwarz, G. 1978, *Ann. Statist.*, 6, 2
- Shakura, N. I. & Sunyaev, R. A. 1973, *A&A*, 24, 337
- Stanek, K. Z. 1996, *ApJ*, 460, L37
- Udalski, A., Szymanski, M., Kubiak, M., et al. 2000, *Acta Astronomica*, 50, 307
- van Hamme, W. 1993, *AJ*, 106, 5
- van Leeuwen, F. 2007, *Astrophysics and Space Science Library*, 350
- Walker, A. R. 2012, *Ap&SS*, 341, 43
- Walker, G. A. H., & Morris, S. C. 1968, *AJ*, 73, 772
- Wyrzykowski, L., Kozłowski, S., Skowron, J., et al. 2009, *MNRAS*, 397, 3
- Zaritsky, D., Harris, J., Thompson, I. B., et al. 2004, *AJ*, 128, 1606
- Zebrun, K., Soszynski, I., Wozniak, P. R., et al. 2001, *Acta Astronomica*, 51, 317